A new design for friction stir spot joining of Al alloys and carbon fibre reinforced composites

Journal:	*Journal of Materials Engineering and Performance*
Manuscript ID	JMEP-20-06-20699.R1
Manuscript Type:	Technical Paper
Date Submitted by the Author:	n/a
Complete List of Authors:	Bolouri, Amir; University of the West of England Bristol Fotouhi, Mohamad; University of Glasgow Moseley, William ; University of the West of England Bristol
Keywords:	Composites, Polymer Matrix, Aluminum, Joining, Friction stir welding, Dissimilar material joining

A new design for friction stir spot joining of Al alloys and carbon fibre reinforced composites

Amir Bolouri[a]

[a] Department of Engineering, Design and Mathematics, University of the West of England (UWE), Bristol BS16 1QY, UK

Mohamad Fotouhi [b]

[b] University of Glasgow, School of Engineering, Glasgow G12 8QQ, UK

William Moseley [a]

[a] Department of Engineering, Design and Mathematics, University of the West of England (UWE), Bristol BS16 1QY, UK

Corresponding author:

Amir Bolouri[a]

[a] Department of Engineering, Design and Mathematics, University of the West of England (UWE), Bristol BS16 1QY, UK

Email address: amir.bolouri@uwe.ac.uk

A new design for friction stir spot joining of Al alloys and carbon fibre reinforced composites

Amir Bolouri [a], Mohamad Fotouhi [b], William Moseley [a]

[a] Department of Engineering, Design and Mathematics, University of the West of England (UWE), Bristol BS16 1QY, UK

[b] University of Glasgow, School of Engineering, Glasgow G12 8QQ, UK

Abstract:

Friction Stir Spot Welding (FSSW) has been recently developed to join dissimilar materials. However, the traditional requirement for a rotating tool consists of a pin and shoulder in FSSW leads to a complex joining process and unpredictable defects. In this study, a new static-shoulder design in FSSW was proposed and developed to join Al alloys to Carbon Fibre Reinforced Polymer (CFRP) composites. The main joining parameters, including pin rotational speed, pin feed rate and pin plunge depth, were varied to investigate their effects on the joining temperature, materials interaction and the strength of joints. The pin rotational speed had the largest influence on the joining temperature. Lap shear tensile testing was conducted to evaluate the performance of the joints. The joints exhibited the ultimate lap shear force from 230 N to 260 N. A brittle fracture occurred with the displacement-at-fracture load of 0.35-0.41 mm. Cross-sectional images revealed the creation of undulations on the surface of Al alloys in the joining zone. The undulations created a macro-mechanical inter-locking bonding between the materials, which determined the performance of the joints. For a flat pin, by increasing the plunge depth from 1.25 mm to 1.30 mm, the undulation size increased from 0.21 mm to 0.26 mm, which can enhance the macro-mechanical interlocking bonding between Al alloys and CFRP

and accordingly increased the ultimate shear force of the joints from 230 N to 241 N. Use of a fluted pin significantly influenced the flow of the plasticized Al alloy in which created pronounced undulations and large Al alloy spikes of 0.46 mm. These features seemed to establish an efficient macro-mechanical interlocking bonding, which resulted in a noticeable improvement in the performance of the joint. For a plunge depth of 1.30 mm, the ultimate shear force increased to 261 N using the fluted pin.

Key words: dissimilar materials joining, friction stir spot joining, Al alloys, composite

1. Introduction

Manufacturers in the transportation sector are constantly seeking to reduce the weight of vehicles [1]. Demanding environmental and economic regulations and policies are forcing companies to increasingly develop and utilise lightweight structures. The conjoined use of dissimilar materials such as light alloys and polymer matrix composites is becoming a progressively popular and common solution [2] [3]. An example of the implementation of hybrid structures (Al alloys and composites) in the automotive industry is the Audi R8, which is 15% lighter than its predecessor whilst boasting a 40% improvement in torsional rigidity. The joining of metals and composites is very challenging due to their highly dissimilar properties [4] [5] [6]. Current traditional forms of joining methods have their drawbacks including being costly and not being environmentally friendly and having a limited performance [7]. For example, mechanical fastening involves holes in the composites which causes major concerns over stress concentrations and interrupts/severs the fibres' continuity [8]. More critically, due to the high notch sensitivity of polymers, the hole drilling raises concerns about crack initiation in the polymer matrix and resultant premature joint failure [7]. Adhesive bonding requires intensive surface treatment of the

surfaces to be bonded, without which the mechanical performance of the joints is very limited [9]. In theory, adhesive bonding is the optimum technique for joining composites, as it provides a uniform stress distribution along the joint, but difficulties in controlling the bond quality limit its practical application [10][11]. Therefore, there is a growing demand for solutions to the challenge of joining metals and composites.

Welding-based techniques are relatively new alternatives to join metals and polymer matrix composites. Principally, in these techniques, the polymer matrix partially remelts that produces a joint with a metallic member after consolidation [12]. Depending on the heat source to remelt the polymer matrix several processes have been used including induction welding [13], resistance spot welding [14][15], ultrasonic welding [16][17] and laser welding [18][19]. Friction stir welding-based processes have also attracted growing interest due to the energy efficiency and environmental friendliness [20]. For example, Friction Spot Joining (FSpJ) has been developed and patented by Helmholtz-Zentrum Geesthacht to spot weld sheet light alloys to Carbon Fibre Reinforced Polymer (CFRP) composites [21]. Feasibility studies have been conducted to manufacture hybrid light metal-CFRP overlap joints [22]–[25]. The process involves simultaneous rotation of a sleeve and pin on the overlapped joining elements of sheet metal and composite, which are fixed using a clamping ring. Initially, the rotating sleeve is plunged into the metallic member to a pre-set depth, while the rotating pin is slightly pulled back. The friction between the sleeve and metal generates heat around the joining zone. A volume of metal is plasticize, which flows it into the space created by the pulled back pin. In the second step, while the sleeve is still rotating in contact with the metal, the pin pushes back the plasticized metal into the composite, creating an undercut shape in the form of a metallic nub. The nub creates a macro-mechanical interlocking bonding between the

metal and composite [26]. In addition, due to the transfer of heat from the metal to the composite, the polymer matrix of a composite can remelt. The reconsolidation of molten polymer under pressure will induce adhesive bonding between the metal and the composite. Although the mechanical properties of manufactured joints are promising, the process seems quite costly and as it requires a tool made of three separate elements, which must rotate and act independently. Furthermore, it seems complex to establish a solid control on the large number of joining parameters in FSpJ.

Conventional Friction Stir Spot Welding (FSSW) processes have been recently employed and adopted to join dissimilar materials [20] [27]. The process has a simpler tooling set up and is less complex to operate compared to FSpJ. In the conventional FSSW, the assembly of rotating tool consists of a shoulder with a pin on its surface [28][29]. During the joining process, while two sheet materials are clamped to form a lap joint, the rotating tool is plunged into the top material of the joint creating heat through both friction and plastic deformation [30]. Consequently, the material becomes plasticized and pin penetrates into the materials and stir them together while shoulder provides further friction and pressure to form the weld. Common defects in the FSSW of metals includes weld thinning and keyhole defects [31]. It has been proposed that use of a static-shoulder can minimize the weld thinning defect [32]. A simplified cylindrical tool design has been used to produce high strength joints and eliminate the keyhole defect [33][34]. In this design, the rotating cylindrical tool creates heat and pushes the plasticized metal into the bottom plate. For the FSSW of metals and polymer matrix composites, the main bonding mechanism is the penetration of a nub of plasticized metal into composites, creating a macro-mechanical inter-locking [24]. A common defect in the FSSW of the metals

and composites is broken stir zone in which the metal under the pin is broken due to the excessive penetration of the tooling [22]. The rotational speed of the pin has also a critical role in determining the properties of joints [35][36]. For example, the high rotational speeds can easily overheat the joining zone [37][38]. In order to minimize the manufacturing defects and create a consistent bonding between metals and polymer matrix composites, it requires designing new setups to make the process much simpler and create a reliable control on the processing parameters.

In this study, a shoulder-less tool design of FSSW is developed and tested for joining Al alloys and CFRP. The aim of this design is that the rotating cylindrical pin pushes a plasticized Al alloy into CFRP to make a nub of the plasticized Al alloy and create a macro-mechanical inter-locking between the Al alloy and CFRP. This can also avoid the keyhole defect in the FSSW process [39]. The generated heat during the friction will be enough to remelt the polymer matrix to wet the interface between the Al alloy and CFRP. The design is further modified by adopting a static-shoulder design. In order to alter the shape of the nub and enhance the macro-mechanical inter-locking, a profiled pin is used. The effects of joining parameters on the strength of joints are discussed and linked to bonding mechanisms.

2. Materials and experimental procedure

Commercially available 2 mm thick rolled 1050 Al alloy plates and unidirectional prepreg CFRP composites with a 50% fibre volume fraction were used for this study. The total thickness of CFRP composite plates was 2 mm. To conduct the joining process, a jig compatible with a conventional CNC milling machine was designed. Figure 1 shows the schematics of jig design and its dimensions. The load cells were attached to the underside of the jig via two M8 clearance holes as shown in Figure 1(a). A 30 mm wide grove with the depth of 3.5 mm running the length of the jig base

was the area in which the Al alloy and CFRP plates were located in a single lap joint configuration. The cumulative depth of the single lap joint of the Al alloy and CFRP was 4 mm, which was larger than the depth of the groove. Therefore, the samples were clamped in a fixed position. Spacers were used to ensure that the samples remained horizontal and clamping pressure was distributed uniformly. A fixed clamping pressure of 0.7MPa was applied during the joining process. The temperature at the joint zone was monitored by using a thermocouple embedded at the interface of CFRP and Al alloy plates. During the joining, the access for the thermocouple was provided as shown in Figure 1(b).

3. Design development

A shoulder-less design of FSSW was used to conduct the joining process. For this design, there was a 4 mm clearance between the pin and the central hole in the lid of the jig. Therefore, only the rotating pin was in contact with the plasticized Al alloy in the joint zone. Using the shoulder-less design, the preliminary experiments failed to establish a consistency in the manufacturing of joints. The most prominent shortcoming of the shoulder-less design was due to the loss of heat and the temperature control in the stirring zone. On the other hand, as shown in Figure 2(a), the expulsion of displaced Al alloy around the pin was occurred during the joining process indicating that Al alloy was moved upwards instead of being pushed into CFRP. Figure 2(b) shows the cross-sectional view of a joint with the expelled Al alloy. It can be assumed that the hot plasticized Al alloy was displaced into the clearance between the rotating pin and the central hole in the lid. The overflow of the plasticized Al alloy also results in the weld thinning defect [31]. This can be seen in Figure 2 (b) by comparing the thickness of the joint zone and the base Al alloy.

In order to solve issues related to the shoulder-less design, a static-shoulder design of FSSW was developed for testing. As shown in Figure 3, a phosphor bronze flanged bushing was installed into the 4 mm clearance between the pin and the central hole in the lid. Therefore, in the joint zone, the plasticized Al alloy was in direct contact with the rotating pin and the static shoulder (the bush). The phosphor bronze was selected because it is well suited for high temperature and high-speed applications. Using the static-shoulder design of FSSW, a consistency in the manufacturing of the joint was established due to simultaneously achieving the accurate control of temperature and increasing the joining temperature to 400 °C. The static-shoulder prevents the overflow of the plasticized Al alloy that can also minimize the weld thinning defect in the FSSW of dissimilar materials [32] [40]. Therefore, the amount of the expelled Al alloy considerably decreased indicting that the more plasticized Al alloy was forced into CFRP. In comparison with the conventional FSSW that the pin height limits the penetration depth and the pin feed rate, for the static-shoulder design in this study, the pin is free to move that provides more flexibility to adjust the joining parameters. The effects of joining parameters on the joining temperature and the properties of joints are discussed in the following sections.

4. Effects of processing parameters on joining temperature

Figure 4 shows the effects of FSSW parameters on the temperature at the joining interface. For different pin rotational speeds, the temperature evolutions are shown in Figure 4 (a). It can be seen that the temperature rapidly increases and reaches the maximum after ~4 sec of joining time. As it is demonstrated in Figure 4 (c), by increasing the rotational speed from 2500 rpm to 3000 rpm, there is a significant increase in the average maximum temperatures from 310 °C to 400 °C.

For these experiments, the plunge depth and the pin feed rate were fixed at 0.8 mm and 12 mm/min, respectively. The rotation was stopped immediately after the plunge depth was obtained without any dwell times. As shown in Figure 4 (b) and (d), by changing the pin feed rate from 7.5 mm/min to 15 mm/min, the average maximum temperature at the joint interface increases from 331 °C to 372 °C. The thermal model of Eq. 1 for heat generation in FSSW can be used to explain these results [24][41].

$$Q = \sum_{n=1}^{N} M(n)\omega(n)\Delta t \quad (1)$$

Q is the generated heat in FSSW, M is the torque (N.m), ω is the rotational speed (rad/s) of tooling, Δt is the joining time, and N is the number of experiments. It can be seen from the equation that rotational speed has a direct influence on the generated heat in which increasing the rotational speed increases heat. In practice, increasing the pin rotational speed increases the pin movement against the Al alloys, which creates more friction between them and generates more heat. Therefore, the temperature at the joining interface increases by increasing the pin rotational speed. The effect of pin feed rate on the generated heat is not directly reflected in the equation. When the pin feed rate is increased, a target pin plunge depth is reached in a shorter time. In other words, for a constant pin plunge depth, the total joining time is shorter when the pin feed rate is higher. For example, for the plunge depth of 0.8 mm, the joining time for the pin feed rate of 7.5 mm/min is 6.4 sec while it is 3.2 sec for the pin feed rate of 15 mm/min. On the other hand, reaching a constant pin plunge depth in a shorter time (a higher pin feed rate) requires more downward axial force on the Al alloy beneath the pin for faster penetration. This increases the applied torque (N.m) by the pin during joining. Therefore, it can be suggested that

based on the equation, the increase in the pin feed rate has two opposing effects on the generated heat: (1) it increases heat through the increased torque (M), and (2) the reduced joining time (Δt) reduces heat. However, their global effect is to increase the generated heat as there is a rise in the average maximum temperature at the interface of Al alloy and CFRP by changing the pin feed rate. This may imply that the effect of force on the generated heat is more dominant than the effect of joining time. S.M. Goushegir et al. have observed similar trend that the axial force has the highest impact on the process temperature, creating larger areas of molten polymer [24].

The influence of pin plunge depth on the joining temperature is demonstrated in Figure 4(d). The plunge depth was increased from 0.8 mm to 1.0 mm for the fixed rotational speed of 2750 rpm and the pin feed rate of 15 mm/min. It can be seen that the temperature slightly increases from 372 °C to 384 °C. To reach a deeper plunge depth at a constant feed rate requires a longer joining time. Specifically, the joining time for the plunge depth of 0.8 mm was ~3 sec while it was ~4 sec for 1.0 mm. Therefore, it enhances the generated heat due to friction (based on Eq. 1) that increases the temperature at the interface of the Al alloy and CFRP.

A dwell time was not implemented in the joining process of above-mentioned experiments. In principal, the dwell time increases the joining time. To examine its effect on the temperature change, a dwell time of 2 sec was implemented into a series of experiments at 2500 rpm rotational speed. When the target plunge depth of 0.8 mm was reached (which was after ~4 sec at the pin feed rate of 12 mm/min), the rotation of pin was continued for additional 2 sec. This increased the joining time from ~4 sec to ~6 sec. The effect of 2 sec dwell time on the temperature change is depicted in Figure 4(c). Although according to Eq. 1 for a longer joining time, a rise in the temperature was excepted due to the increased heat generation, the change in

the temperature is negligible compared to experiments without the dwell time. This behaviour may be explained due to the tool slip, which is commonly observed in FSSW of Al alloys [42]. It is discussed that at the high temperatures during joining, the viscosity of plasticized Al alloys is reduced [22] [42]. Therefore, it could be assumed that the pin tool slips over the soft plasticized Al alloy during the dwell time (the prolonged joining time). Consequently, no additional heat can be created between the pin and the Al alloy due to the friction. It is of great importance to mention that the joining time has a direct control on the generated heat and consequently on the joining temperature in FSSW processes as discussed earlier. However, it has been discussed that the prolonged joining time may have a complicated effect on the FSSW joining of the Al alloys and CFRP due to highly dissimilar characteristics of materials creating a complex interaction between them [22] [24].

5. Manufacturing of Al alloy and CFRP joints

As discussed earlier, for the rotational speeds of less than 3000 rpm, the joining temperatures are below 400 °C. It is observed that at the low joining temperatures, the tackiness of the plasticised Al alloy increases, which causes the Al alloy sticks to the pin and be ripped from the stir zone as the pin recedes. This creates broken stir zone (BSZ) defect that is a common defect in FSpJ of Al alloys and CFRP [22]. Therefore, in order to obtain the temperatures above 400 °C at the joining interface, the pin rotational speed of 3000 rpm is selected for the rest of this study.

The process parameters, including plunge depth, joining time and pin feed rate [14], and tool designs [39] have significant influences on the bonding between materials in the FSSW process. In the following sections, their influence on the joining of the Al alloy and CFPR, and the performance of the joints are discussed.

5.1. Effects of process parameters on joining mechanisms

Table 1 summarises observations for the effect of processing parameters on the joining of the Al alloys and CFRP. For each condition, a minimum of five experiments was conducted for the evaluation of repeatability and consistency. For a small plunge depth of 0.75 mm, the joining between the Al alloys and CFRP was unsuccessful. On the other hand, the change in the pin feed rate – which influences joining time and force – did not show any impact on the joining. Increasing the plunge depth to 1.25 mm established the joining between the Al alloy and CFRP. By changing the pin feed rate from 2.5 mm/min to 12 mm/min the repeatability and consistency in joining were considerably improved. A typical example of a sound Al alloy and CFRP joint is shown in Figure 5(a). Further increasing the plunged depth to 1.50 mm did not appeared beneficial for the joining. For these joints, by increasing the pin feed rate from 2.5 mm/min to 5.0 mm/min, although the joining was obtained, the repeatability was very poor and BSZ defect occurred. In addition, the change in the pin feed rate to 7.5 mm/min and 12 mm/min further gave rise to the BSZ defect (Figure 5(b)) and the joining was not obtained. It appears that the plunge depth of 1.50 mm introduced an excessive penetration of the pin that broke and removed the Al alloy beneath the pin and created the BSZ defect. Furthermore, in these joints, increasing the pin feed rate increased the axial force on the Al alloy that aggravated the occurrence of the BSZ defect.

It has been discussed in the literature that the adhesive bonding and macro-mechanical inter-locking between Al alloys and CFRP are the major bonding mechanisms in the friction stir spot joining processes [22] [23]. The reconsolidation of re-melted polymer matrix in contact with the Al alloy creates the adhesive bonding between Al alloys and CFRP. The macro-mechanical inter-locking between Al alloys

and CFRP occurs due to the formation and penetration of a nub of plasticised Al alloy that penetrates into CFRP creating the inter-locking [23]. For the joining with 0.75 mm plunge depth, it seems that the penetration is not sufficient to create the macro-mechanical interlocking. On the other hand, despite the evidence of wetting the Al alloys by molten polymer matrix (Figure 5 (c)), the adhesive boning between materials was not obtained or it was very weak to hold the materials together for these joints. As discussed earlier, at the rotational speed of 3000 rpm, the generated heat due to the friction is sufficient to rise the temperature above 400 °C that re-melts a thin layer of polymer matrix and wets the interface of the Al alloy and CFRP [24].

The establishment of bonding between the Al alloy and CFRP for the increased plunge depth of 1.25 mm can be explained based on the increase in the penetration of plasticised Al alloy nub into CFRP that enhances the macro-mechanical interlocking boning mechanism. To understand the effect of change in the plunge depth of 1.25 mm on the macro-mechanical inter-locking at the interface of the joints, a series of joints were manufactured within a plunge depth of 1.25-1.35 mm to ensure a successful joining. The joints were fully mounted in resin and were cut using a water jet cutting for cross-sectional investigations. The cross-sectional views are shown in Figure 6 (a) and (b) for Al alloy and CFRP joints with different plunge depths. From these cross-sectional views, the deformation and penetration of the Al alloy into CFRP at the joint interface are visible. The plasticized Al alloy undergoes high shear rates at the high temperature of ~400 °C due to the rotation and downward force of pin, which cause the plasticized Al alloy to deform and flow [34]. The interaction of the plasticized Al alloy and high stiff CFRP creates the nub with undulation features at their interface during the joining process. The axial force is

expected to penetrate the nub of the plasticized Al alloy into the CFRP. However, due to the high stiffness of CFRP, it is less likely that a considerable penetration of the nub into CFRP could be obtained in the joining. By comparing Figure 6 (a) and (b), it is evident that with increasing the plunge depth from 1.25 mm to 1.30 mm, the deformation zone increases in depth with larger undulations, penetrating into layers of the CFRP. To estimate the penetration of the nub, the size of the undulations was measured using an optical microscope equipped with a digital image analyser. For different conditions, the average size of the undulations is summarized in Table 2. The undulation size is 0.26±0.07 mm for the plunge depth of 1.30 mm, which is %20 larger compared to the undulation size of 0.21±0.05 mm for the plunge depth of 1.25 mm. The larger undulations can indicate that the penetration of the plasticized Al alloy is deeper that enhances the macro-mechanical interlocking between the Al alloy and CFRP [43], [44].

5.2 Effect of pin profile on joining mechanisms

Figure 6(c) shows a typical cross-sectional view of the Al alloy and CFRP joint manufactured using a fluted pin. In comparison with a flat pin (Figure 6 (b)), it is evident that the fluted pin considerably increases the deformation of the Al alloy in the joining zone. For example, there is one main circumferential undulation at the periphery of the stir zone, appearing as large Al alloy hooks (Figure 6(c)). With the fluted pin, the flow of the plasticized Al alloy is radially toward the middle of the joining zone, which is driven by the flutes on the pin [39]. By conservation of volume, this pushes more plasticized Al alloy downwards, increasing the nub penetration and deformation. In contrast, with the flat pin, the flow of the plasticized Al alloy is not inwards, creating less deformation and penetration. A similar behaviour has been observe by D. Bakavos et al. [39] and A. Reilly et al. [34] for FSSW of dissimilar Al

alloys, who also proposed that the pin surface profile changes the flow behaviour of the plasticized Al in the joining. In comparison with the flat pin, the average size of undulations is ~40% larger for the fluted pin (Table 2), which indicates more penetration of the nub into the CFRP, enhancing the macro-mechanical inter-locking. On the other hand, the radial flow of the Al alloy near the top surface in the interaction with stiff CFRP layers creates large circumferential hooks.

5.3. Performance of the joints

Figure 7 shows the effect of the plunge depth and pin surface profile on the lap shear strength of the joints. The pin feeding rate and the rotational speeds were fixed at 12 mm/min and 3000 rpm, respectively. The lap shear tensile tests were conducted according to standard ASTM D3163 using an Instron 4204 electro-mechanical testing system with a cross-head speed of 1.27 mm/min. The ultimate shear force was extracted from the force–displacement graphs. It is clear that the influences of the plunge depth and pin profile on the characteristics of joint interfaces are reflected on their strength (Figure 7). As discussed in section 5.1, the plunge depth influences the shape and size of the plasticized Al alloy nub and undulations and therefore, the macro-mechanical inter-locking bonding between the Al alloy and CFRP. Larger undulations size and penetration depth of the Al alloy nub into the CFRP enhances the macro-mechanical interlocking between the materials and strength of the joints. The increase in the plunge depth from 1.25 mm to 1.3 mm increases the undulation size of the Al Alloy by 20% (Table 2) and the penetration depth of the Al alloy nub into CFRP, which increase the macro-mechanical inter-locking. On the other hand, from the cross-sectional views of joints (Figure 6 (a) and (b)), it appears that for the joints manufactured with the plunge depth of 1.30 mm, the undulations with a larger profile height on the Al alloys surface are in interaction with

CFRP. This leads to the increased inter-locking surface area and the amount of inter-locked material in the joint zone. Consequently, the lap shear strength of the joints slightly increases from 230 N to 241 N by increasing the plunge depths from 1.25 mm to 1.30 mm (Figure 7).

The joints manufactured by the fluted pin exhibits noticeably higher lap shear strengths compared to the joints manufactured using the flat pin (Figure 7). With the fluted pin, the deformation of the Al alloy becomes severe, leading to the hooking behaviour at the joint interface (Figure 6 (c)), and the significant increases in the size of undulations and the penetration of the plasticized Al alloy nub into the CFPR compared to the flat pin (Table 2). Larger nub penetration and undulations increase the macro-mechanical inter-locking between the materials. Furthermore, the hooking builds up additional macro-mechanical inter-locking between the Al alloys and CFRP. The hooks noticeably retain the CFRP attached with the Al alloys, which can increase the strength of joints. In addition, as a result of the creation of more pronounced nub and hooks, the intimate contact at the interface of the Al alloy and CFRP increases that can further push the molten resin to fill into the crevices on the surface of the Al alloy. This can generate a micro-mechanical inter-locking between materials [23]. The surface profile of materials has been identified as one of the key parameters to enhance the mechanical interlocking in the joining of composites [44], [45]. Therefore, with the fluted pin, the features at the interface of joints can create efficient mechanical interlocking mechanisms between the materials that increases the lap shear strength of joints from 230 N to 261 N. The application of surface treatments such as porous structures on the surface of the Al alloy or a combined use friction self-riveting welding can further increase the strength of the joints[36].

Figure 8 shows the typical force-displacement curves for the lap shear tests of the joints manufactured by the flat and fluted pins for the 1.25 mm plunge depth. The displacement-at-fracture load is a very small value of 0.35 mm for the flat pin and 0.41 mm for the fluted pin, which clearly indicates a brittle failure behaviour of the joints. In general, this is due to the inelastic nature of interlocking between the materials. However, for the fluted pin, the efficient macro-mechanical interlocking between the Al and CFRP (Figure 6 (c)) may cause plastic deformation on the Al alloy hooks in the joining zone, which increases the displacement-at-fracture load to 0.41 mm.

For displacements less than ~0.10 mm, the rate of increase in the shear force as a function of the displacement appear irregular with slow and sharp increases. This anomaly is likely to have occurred due to the slippage of the joint interface, whilst still maintaining its interlock, allowing the force to further increase. In other words, this might suggest that initially, the joint settles and the joint interface interlocks. After this point (the displacements above ~0.1 mm), the linear correlations between the force and the displacement appear before the final fractures occur at the peaks.

6. Conclusions

The feasibility of using a static-shoulder design for FSSW to join the Al alloys and CFRP is successfully demonstrated. Compared to the advanced FSpJ, the static-shoulder friction welding design provides a simpler manufacturing process to produce the Al alloy and CFRP joints. The increase in the rotational speed of the pin from 2500 rpm to 3000 rpm increases the joining temperature by approximately 95-105 °C. The changes in the pin plunge depth and pin feed rate show a moderate effect on the joining temperature. The cross-sectional views at the joining zone show

that CFRP is embedded into undulations on the surface of the deformed Al alloy. For the flat pin, the increase in the pin plunge depth from 1.25 mm to 1.30 mm slightly increases the undulation size and the penetration of plasticized Al alloy nub, which promotes the macro-mechanical interlocking between the Al alloy and CFRP. Consequently, the ultimate lap shear force moderately increases by 10 N for a higher plunge depth of 1.30 mm. The use of the fluted pin noticeably increases the undulation size with a hooking behaviour of the Al alloy at the interface of the joints, which can create a more efficient macro-mechanical interlocking between the Al alloy and CFRP and accordingly significantly increases the performance of the joints. The force-displacement for shear tests shows a brittle fracture for the joints.

Acknowledgments

The authors would like to acknowledge the financial support from the University of the West of England through Vice Chancellors Interdisciplinary Research Challenge Fund 19/20.

References

[1] G. Davies, “Future trends in automotive body materials,” in *Materials for Automobile Bodies*, 2003.

[2] P. K. Mallick, *Materials, design and manufacturing for lightweight vehicles*. 2010.

[3] K. Matsuyama, “Trend of automobile vehicles and the joining technologies,” *Riv. Ital. della Saldatura*, 2007.

[4] M. Grujicic *et al.*, “The potential of a clinch-lock polymer metal hybrid technology for use in load-bearing automotive components,” *J. Mater. Eng.*

Perform., 2009.

[5] P. Woizeschke and F. Vollertsen, “Fracture Analysis of Competing Failure Modes of Aluminum-CFRP Joints Using Three-Layer Titanium Laminates as Transition,” *J. Mater. Eng. Perform.*, 2015.

[6] F. Faupel, R. Willecke, and A. Thran, “Diffusion of metals in polymers,” *Mater. Sci. Eng. R Reports*, 1998.

[7] S. T. Amancio-Filho and J. F. Dos Santos, “Joining of polymers and polymer-metal hybrid structures: Recent developments and trends,” *Polym. Eng. Sci.*, vol. 49, no. 8, pp. 1461–1476, 2009.

[8] F. Hirsch, S. M??ller, M. Machens, R. Staschko, N. Fuchs, and M. K??stner, “Simulation of self-piercing rivetting processes in fibre reinforced polymers: Material modelling and parameter identification,” *J. Mater. Process. Technol.*, vol. 241, pp. 164–177, 2017.

[9] C. Tornow *et al.*, “Quality assurance concepts for adhesive bonding of composite aircraft structures – characterisation of adherent surfaces by extended NDT,” *J. Adhes. Sci. Technol.*, vol. 29, no. 21, pp. 2281–2294, Nov. 2015.

[10] S. Pawlak, “Application of IR Thermography with Thermal Diffusivity Analysis for Detection of Plies Displacement in CFRP Composites,” *J. Mater. Eng. Perform.*, 2018.

[11] D. N. Markatos, K. I. Tserpes, E. Rau, S. Markus, B. Ehrhart, and S. Pantelakis, “The effects of manufacturing-induced and in-service related bonding quality reduction on the mode-I fracture toughness of composite

bonded joints for aeronautical use," *Compos. Part B Eng.*, vol. 45, no. 1, pp. 556–564, 2013.

[12] A. Pramanik *et al.*, "Joining of carbon fibre reinforced polymer (CFRP) composites and aluminium alloys – A review," *Composites Part A: Applied Science and Manufacturing*. 2017.

[13] P. Mitschang, R. Velthuis, and M. Didi, "Induction spot welding of metal/CFRPC hybrid joints," *Advanced Engineering Materials*. 2013.

[14] M. Okayasu and T. Kubota, "An Electrical Resistance Joining Technology for Carbon Fiber-Reinforced Polyphenylene Sulfide Composites," *J. Mater. Eng. Perform.*, 2020.

[15] S. Ren, Y. Ma, S. Saeki, Y. Iwamoto, and N. Ma, "Numerical analysis on coaxial one-side resistance spot welding of Al5052 and CFRP dissimilar materials," *Mater. Des.*, 2020.

[16] F. Lionetto, C. Mele, P. Leo, S. D'Ostuni, F. Balle, and A. Maffezzoli, "Ultrasonic spot welding of carbon fiber reinforced epoxy composites to aluminum: mechanical and electrochemical characterization," *Compos. Part B Eng.*, 2018.

[17] F. Balle, G. Wagner, and D. Eifler, "Ultrasonic metal welding of aluminium sheets to carbon fibre reinforced thermoplastic composites," *Adv. Eng. Mater.*, 2009.

[18] J. P. Bergmann and M. Stambke, "Potential of Laser-manufactured Polymer-metal hybrid Joints," in *Physics Procedia*, 2012.

[19] W. Tao, X. Su, Y. Chen, and Z. Tian, "Joint formation and fracture

characteristics of laser welded CFRP/TC4 joints," *J. Manuf. Process.*, 2019.

[20] G. Buffa, D. Baffari, D. Campanella, and L. Fratini, "An Innovative Friction Stir Welding Based Technique to Produce Dissimilar Light Alloys to Thermoplastic Matrix Composite Joints," *Procedia Manuf.*, 2016.

[21] dos S. J. Amancio Filho ST, "Method for joining metal and plastic workpieces," European Patent EP 2329905 B1, 2012.

[22] J. V. Esteves, S. M. Goushegir, J. F. dos Santos, L. B. Canto, E. Hage, and S. T. Amancio-Filho, "Friction spot joining of aluminum AA6181-T4 and carbon fiber-reinforced poly(phenylene sulfide): Effects of process parameters on the microstructure and mechanical strength," *Mater. Des.*, 2015.

[23] S. M. Goushegir, J. F. dos Santos, and S. T. Amancio-Filho, "Friction Spot Joining of aluminum AA2024/carbon-fiber reinforced poly(phenylene sulfide) composite single lap joints: Microstructure and mechanical performance," *Mater. Des.*, vol. 54, pp. 196–206, 2014.

[24] S. M. Goushegir, J. F. dos Santos, and S. T. Amancio-Filho, "Influence of process parameters on mechanical performance and bonding area of AA2024/carbon-fiber-reinforced poly(phenylene sulfide) friction spot single lap joints," *Mater. Des.*, 2015.

[25] S. M. Goushegir, "Friction spot joining (FSpJ) of aluminum-CFRP hybrid structures," *Weld. World*, 2016.

[26] N. M. André, S. M. Goushegir, J. F. Dos Santos, L. B. Canto, and S. T. Amancio-Filho, "Friction Spot Joining of aluminum alloy 2024-T3 and carbon-fiber-reinforced poly(phenylene sulfide) laminate with additional PPS film

interlayer: Microstructure, mechanical strength and failure mechanisms," *Compos. Part B Eng.*, vol. 94, pp. 197–208, 2016.

[27] F. Yusof, M. R. bin Muhamad, R. Moshwan, M. F. bin Jamaludin, and Y. Miyashita, "Effect of surface states on joining mechanisms and mechanical properties of aluminum alloy (A5052) and Polyethylene Terephthalate (PET) by dissimilar friction spot welding," *Metals (Basel).*, 2016.

[28] R. Ramesh, I. Dinaharan, R. Kumar, and E. T. Akinlabi, "Microstructure and Mechanical Characterization of Friction-Stir-Welded 316L Austenitic Stainless Steels," *J. Mater. Eng. Perform.*, 2019.

[29] R. S. Mishra, M. W. Mahoney, Y. Sato, and Y. Hovanski, *Friction stir welding and processing VIII*. 2016.

[30] B. T. Gibson *et al.*, "Friction stir welding: Process, automation, and control," *J. Manuf. Process.*, 2014.

[31] X. Meng, Y. Huang, J. Cao, J. Shen, and J. F. dos Santos, "Recent progress on control strategies for inherent issues in friction stir welding," *Prog. Mater. Sci.*, 2020.

[32] P. S. Davies, B. P. Wynne, W. M. Rainforth, M. J. Thomas, and P. L. Threadgill, "Development of microstructure and crystallographic texture during stationary shoulder friction stir welding of Ti-6Al-4V," *Metall. Mater. Trans. A Phys. Metall. Mater. Sci.*, 2011.

[33] Y. Tozaki, Y. Uematsu, and K. Tokaji, "A newly developed tool without probe for friction stir spot welding and its performance," *J. Mater. Process. Technol.*, 2010.

[34] A. Reilly, H. Shercliff, Y. Chen, and P. Prangnell, “Modelling and visualisation of material flow in friction stir spot welding,” *J. Mater. Process. Technol.*, 2015.

[35] Y. Huang *et al.*, “Friction stir welding/processing of polymers and polymer matrix composites,” *Composites Part A: Applied Science and Manufacturing*. 2018.

[36] X. Meng *et al.*, “Friction self-riveting welding between polymer matrix composites and metals,” *Compos. Part A Appl. Sci. Manuf.*, 2019.

[37] Y. Huang, X. Meng, Y. Xie, J. Li, and L. Wan, “Joining of carbon fiber reinforced thermoplastic and metal via friction stir welding with co-controlling shape and performance,” *Compos. Part A Appl. Sci. Manuf.*, 2018.

[38] J. Jiao, Z. Xu, Q. Wang, L. Sheng, and W. Zhang, “CFRTP and stainless steel laser joining: Thermal defects analysis and joining parameters optimization,” *Opt. Laser Technol.*, 2018.

[39] D. Bakavos, Y. Chen, L. Babout, and P. Prangnell, “Material interactions in a novel pinless tool approach to friction stir spot welding thin aluminum sheet,” *Metall. Mater. Trans. A Phys. Metall. Mater. Sci.*, 2011.

[40] S. Eslami, T. Ramos, P. J. Tavares, and P. M. G. P. Moreira, “Shoulder design developments for FSW lap joints of dissimilar polymers,” *J. Manuf. Process.*, 2015.

[41] P. Su, A. Gerlich, T. H. North, and G. J. Bendzsak, “Energy generation and stir zone dimensions in friction stir spot welds,” in *SAE Technical Papers*, 2006.

[42] S. Horie, M. Yamamoto, K. Shinozaki, T. H. North, A. Gerlich, and T. Shibayanagi, “Local melting and cracking during friction stir spot welding on

Mg -Al binary alloy," *Yosetsu Gakkai Ronbunshu/Quarterly J. Japan Weld. Soc.*, 2009.

[43] O. P. Ciuca, R. M. Carter, P. B. Prangnell, and D. P. Hand, "Characterisation of weld zone reactions in dissimilar glass-to-aluminium pulsed picosecond laser welds," *Mater. Charact.*, 2016.

[44] R. Tao, M. Alfano, and G. Lubineau, "Laser-based surface patterning of composite plates for improved secondary adhesive bonding," *Compos. Part A Appl. Sci. Manuf.*, 2018.

[45] R. Tao, M. Alfano, and G. Lubineau, "In situ analysis of interfacial damage in adhesively bonded composite joints subjected to various surface pretreatments," *Compos. Part A Appl. Sci. Manuf.*, 2019.

Figure captions:

Figure 1 Schematics of jig design with key dimensions. (a) jig base, 50 mm deep, (b) plan view of the base showing all threaded fixing holes and key dimensions in millimetres, (c) assembled base and lid, pin passing through the lid to contact Al plate.

Figure 2 (a) A joint produced using a shoulder-less design with expelled Al alloy (b) a cross sectional view of expelled Al alloy.

Figure 3 Static-shoulder design for FSSW set-up (a) Phosphor bronze flange bushing and pin, and (b) Phosphor bronze flanged bushing countersunk into the underside of the lid.

Figure 4 Effects of processing parameters on joining temperature (a, b) temperature evolution (c, d) maximum temperature.

Figure 5 Typical examples of (a) Al-CFRP joints produced using 1.25 mm plunge depth at 12 mm/min pin feeding rate, (b) BSZ defect on Al plate, and (c) wetting of Al plate by remelt polymer matrix.

Figure 6 Cross sections of Al-CFRP joints produced using (a) the flat pin design and the plunge depth of 1.25mm, (b) the flat pin design and the plunge depth of 1.30mm, and (c) the fluted pin design and the plunge depth of 1.30mm.

Figure 7 The effect of pin plunge depth and fluted pin design on the lap shear strength of Al-CFRP joints.

Figure 8 Lap shear force-displacement curves for Al-CFRP joints manufactured by flat and fluted pin designs for the plunge depth of 1.25 mm, the pin feeding rate of 12 mm/min and the pin rotational speed of 3000 rpm.

Table captions:

Table 1 Observations and results of joint manufacturing

Table 2 Size of undulations at joint interface

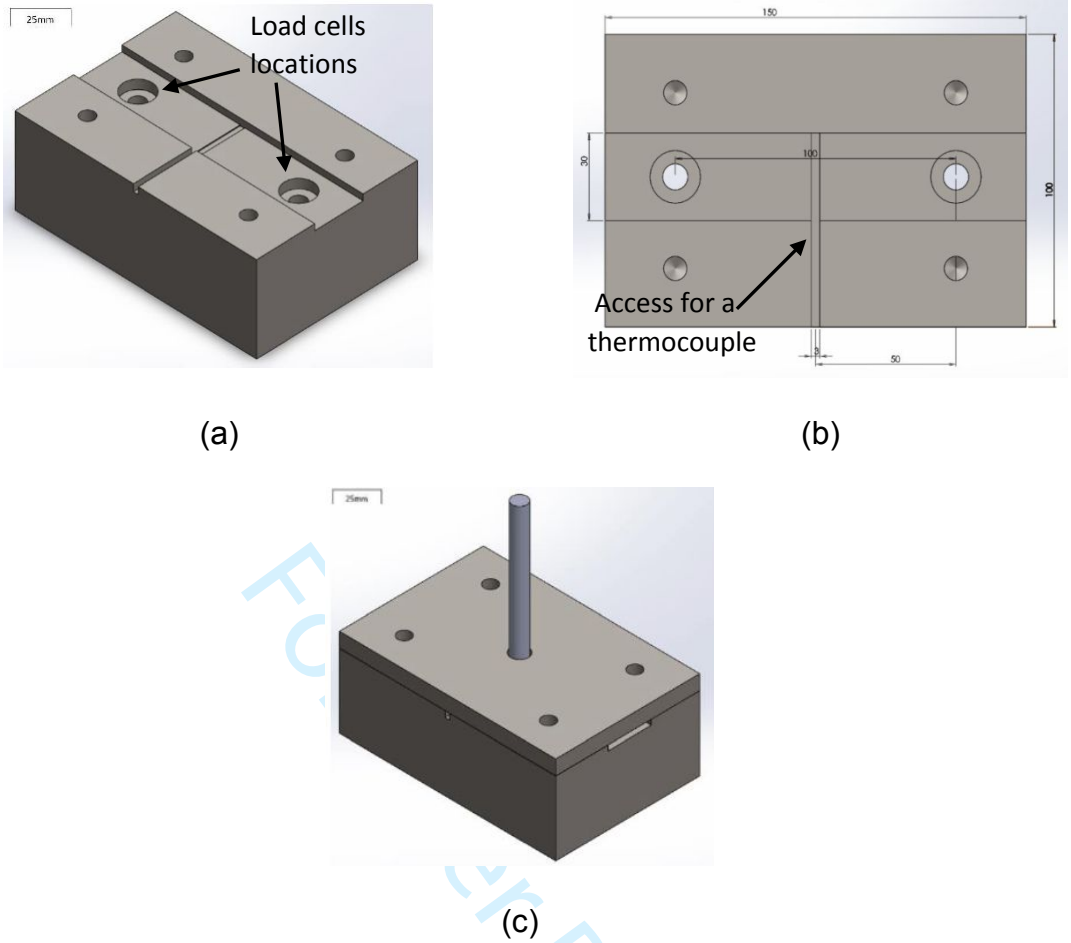

Figure 1 Schematics of jig design with key dimensions. (a) jig base, 50 mm deep, (b) plan view of the base showing all threaded fixing holes and key dimensions in millimetres, (c) assembled base and lid, pin passing through the lid to contact Al.

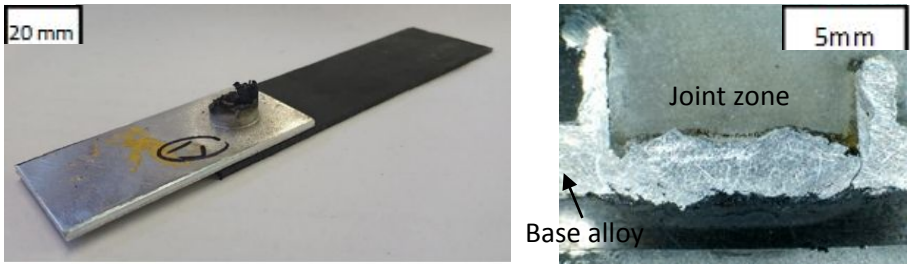

(a) (b)

Figure 2 (a) A joint produced using a shoulder-less design with expelled Al alloy (b) a cross sectional view of expelled Al alloy.

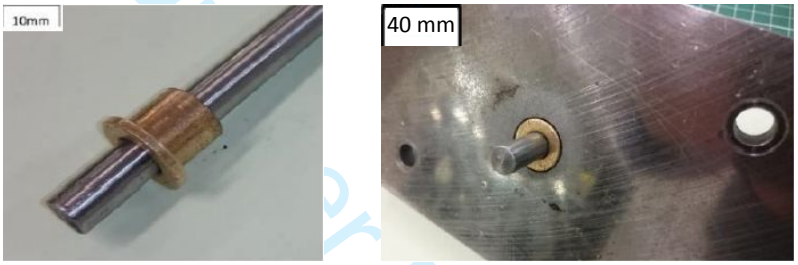

(a) (b)

Figure 3 Static-shoulder design for FSSW set-up (a) Phosphor bronze flange bushing and pin, and (b) Phosphor bronze flanged bushing countersunk into the underside of the lid.

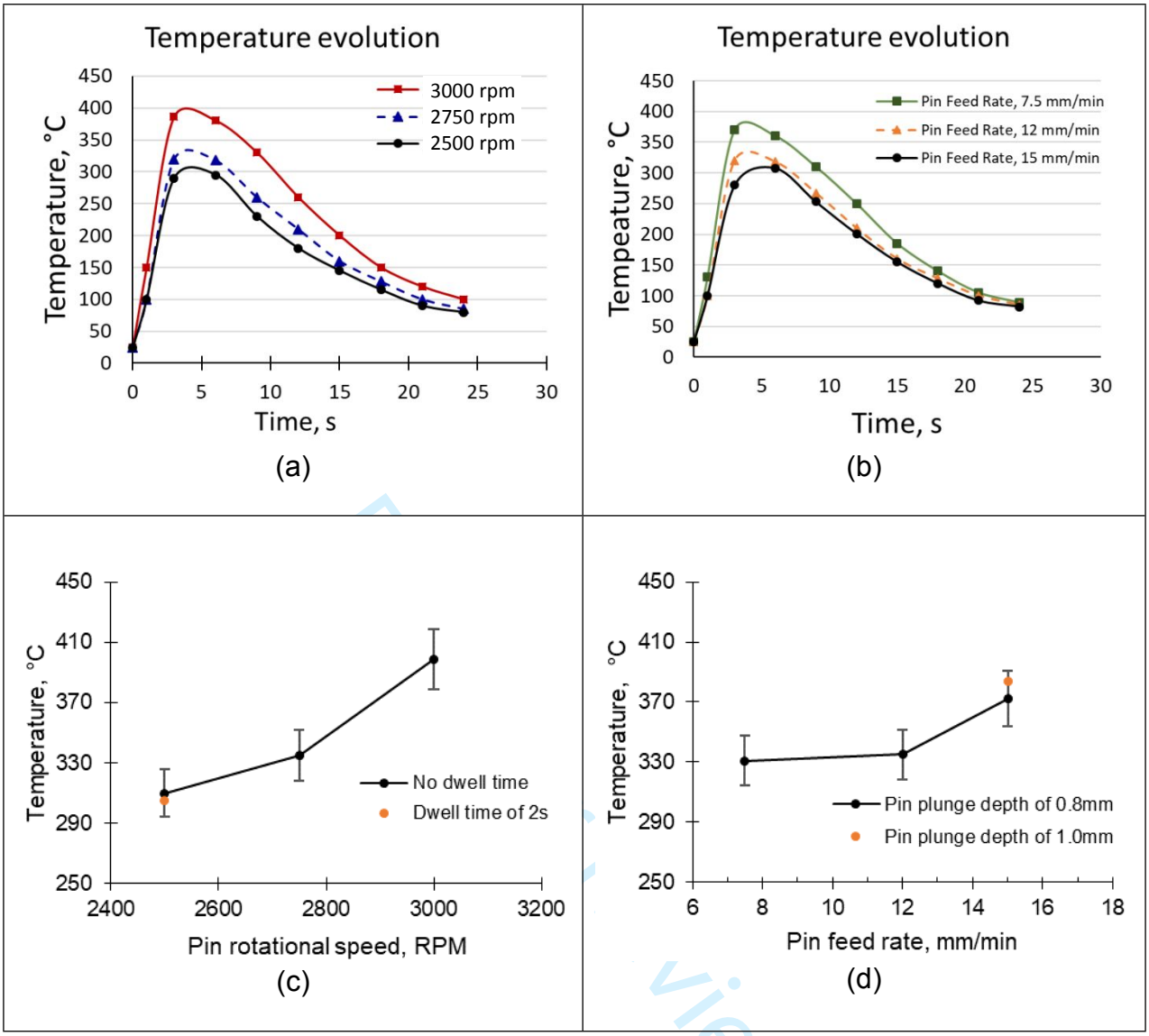

Figure 4 Effects of processing parameters on joining temperature (a, b) temperature evolution (c, d) maximum temperature.

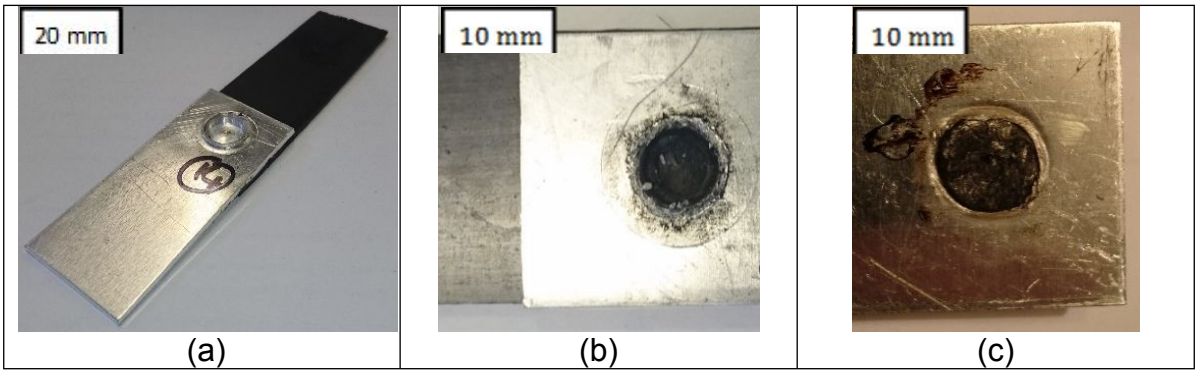

Figure 5 Typical examples of (a) Al-CFRP joints produced using 1.25 mm plunge depth at 12 mm/min pin feeding rate, (b) BSZ defect on Al alloy plate, and (c) wetting of Al plate by remelt polymer matrix.

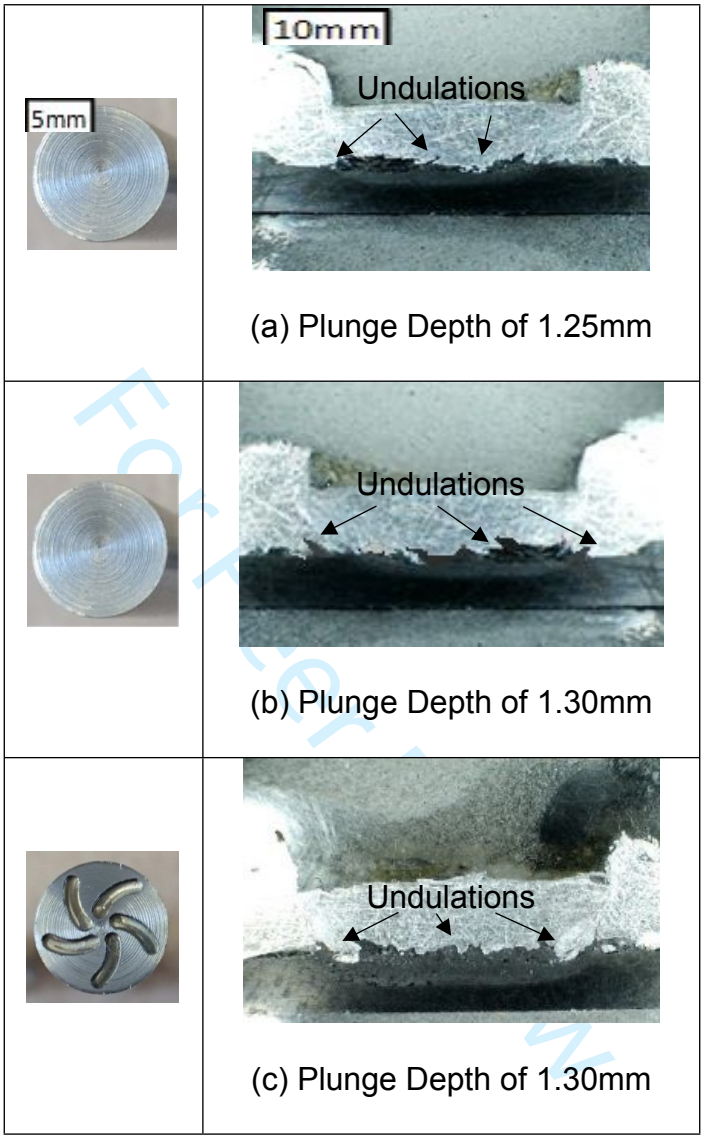

Figure 6 Cross sections of Al-CFRP joints produced using (a) the flat pin design and the plunge depth of 1.25 mm, (b) the flat pin design and the plunge depth of 1.30 mm, and (c) the fluted pin design and the plunge depth of 1.30 mm.

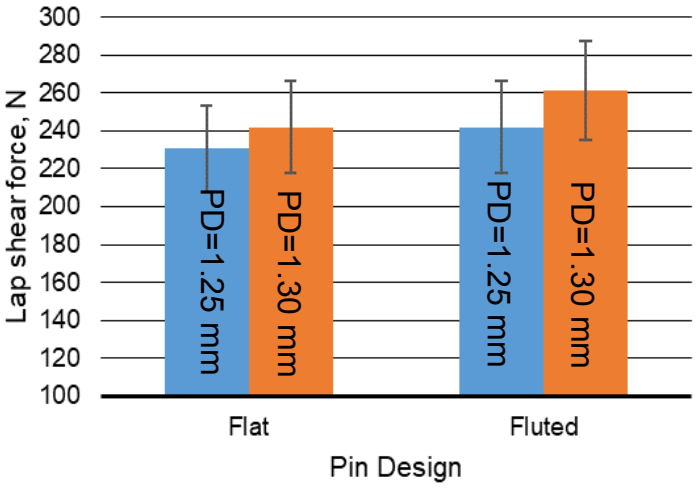

Figure 7 The effect of pin plunge depth (PD) and fluted pin design on the lap shear strength of Al-CFRP joints.

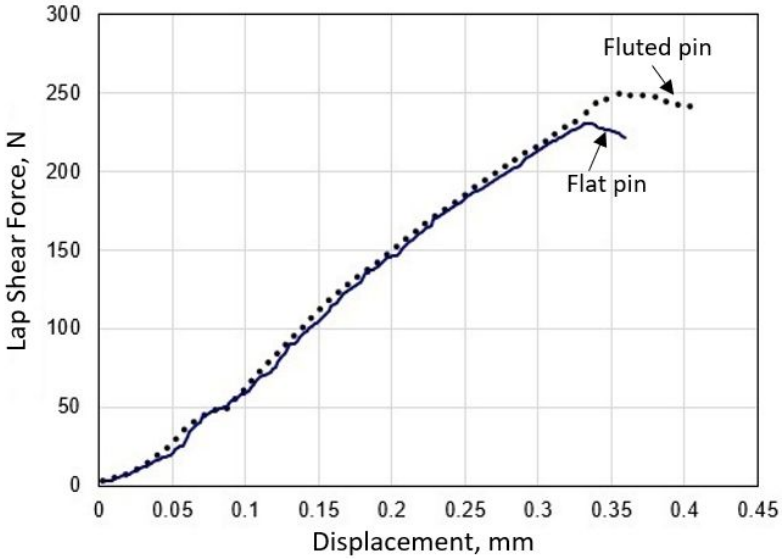

Figure 8 Lap Shear Force-displacement curves for Al-CFRP joints manufactured by flat and fluted pin designs for the plunge depth of 1.25 mm, the pin feeding rate of 12 mm/min and the pin rotational speed of 3000 rpm.

Table 1 Observations and results of joint manufacturing

PD (mm)	FR (mm/min)	Joining	Repeatability
0.75	7.5	No	
0.75	12	No	
0.75	15	No	
0.75	20	No	
1.25	2.5	No	
1.25	5	Yes	Poor (1-2 successful joining out of 5 attempts)
1.25	7.5	Yes	Good (2-3 successful joining out of 5 attempts)
1.25	12	Yes	High (4-5 successful joining out 5 attempts)
1.5	2.5	No	
1.5	5	Yes/BSZ	Poor (1-2 successful joining out of 5 attempts)
1.5	7.5	No/BSZ	
1.5	12	BSZ	

Table 2 Size of undulations at joint interface

Pin surface	Plunge depth, mm	Undulation size, mm
Flat	1.25	0.21±0.05
Flat	1.30	0.26±0.07
Fluted	1.30	0.43±0.10

Table 1 Observations and results of joint manufacturing

PD (mm)	FR (mm/min)	Joining	Repeatability
0.75	7.5	No	
0.75	12	No	
0.75	15	No	
0.75	20	No	
1.25	2.5	No	
1.25	5	Yes	Poor (1-2 successful joining out of 5 attempts)
1.25	7.5	Yes	Good (2-3 successful joining out of 5 attempts)
1.25	12	Yes	High (4-5 successful joining out 5 attempts)
1.5	2.5	No	
1.5	5	Yes/BSZ	Poor (1-2 successful joining out of 5 attempts)
1.5	7.5	No/BSZ	
1.5	12	BSZ	

Table 2 Size of undulations at joint interface

Pin surface	Plunge depth, mm	Undulation size, mm
Flat	1.25	0.21±0.05
Flat	1.30	0.26±0.07
Fluted	1.30	0.43±0.10